Supplement of Geosci. Model Dev., 19, 7303–7323, 2026
https://doi.org/10.5194/gmd-19-7303-2026-supplement

Geoscientific Model Development
Open Access

Supplement of

SPIN (v1.0): A spontaneous synthetic tropical cyclone model empowered by NeuralGCM for hazard assessment

Yurong Gao and Dazhi Xi

Correspondence to: Dazhi Xi (dazhixi@hku.hk)

Contents of this file

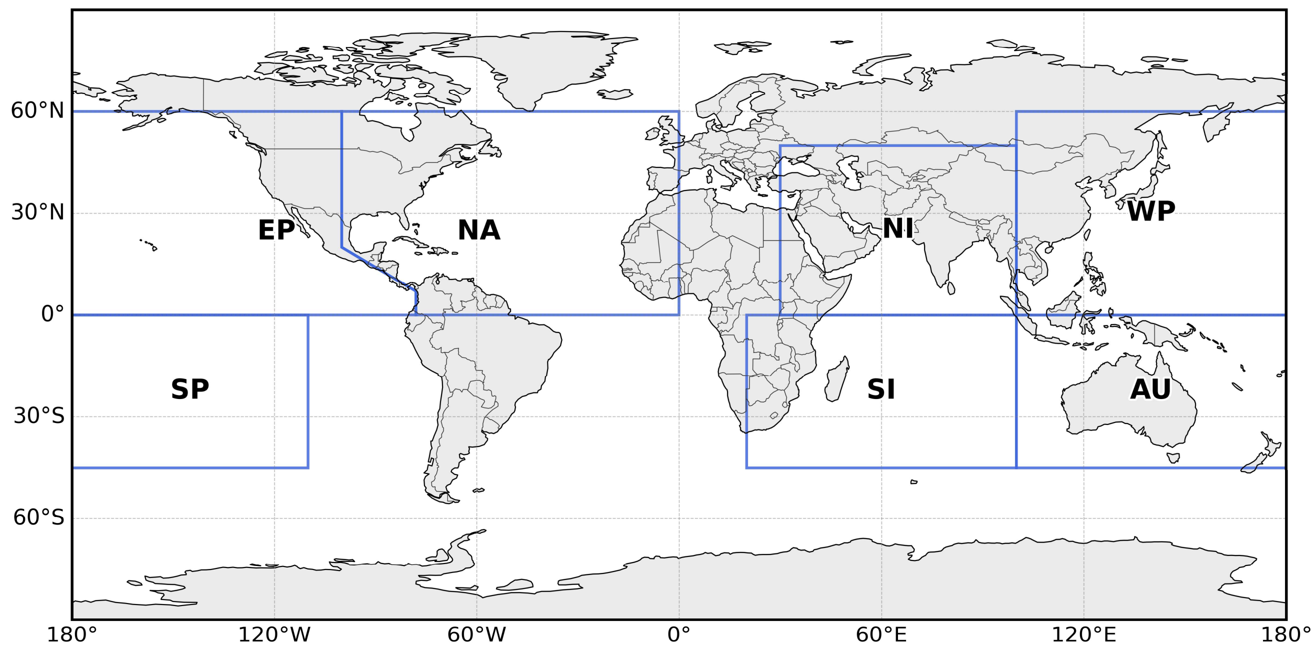

Figure S1. Basin boundaries as defined in this study.

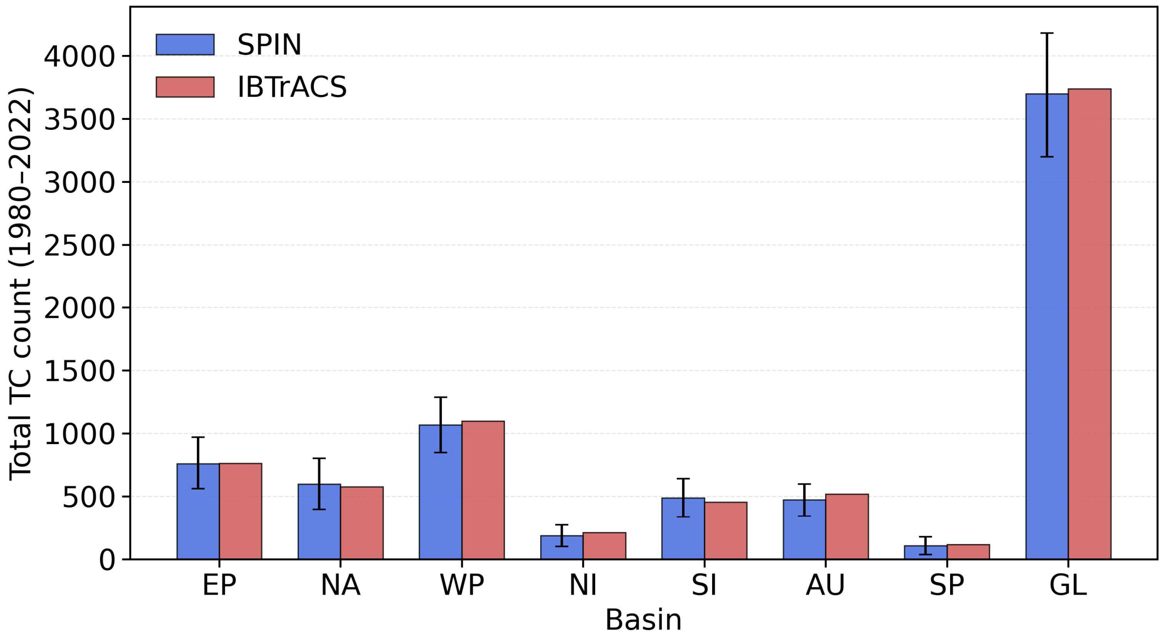

Figure S2. Comparison of total tropical cyclone (TC) counts from 1980–2022 between IBTrACS (red) and the 14-member SPIN ensemble mean (blue) across basins. Error bars indicate the 10–90% ensemble spread for SPIN.

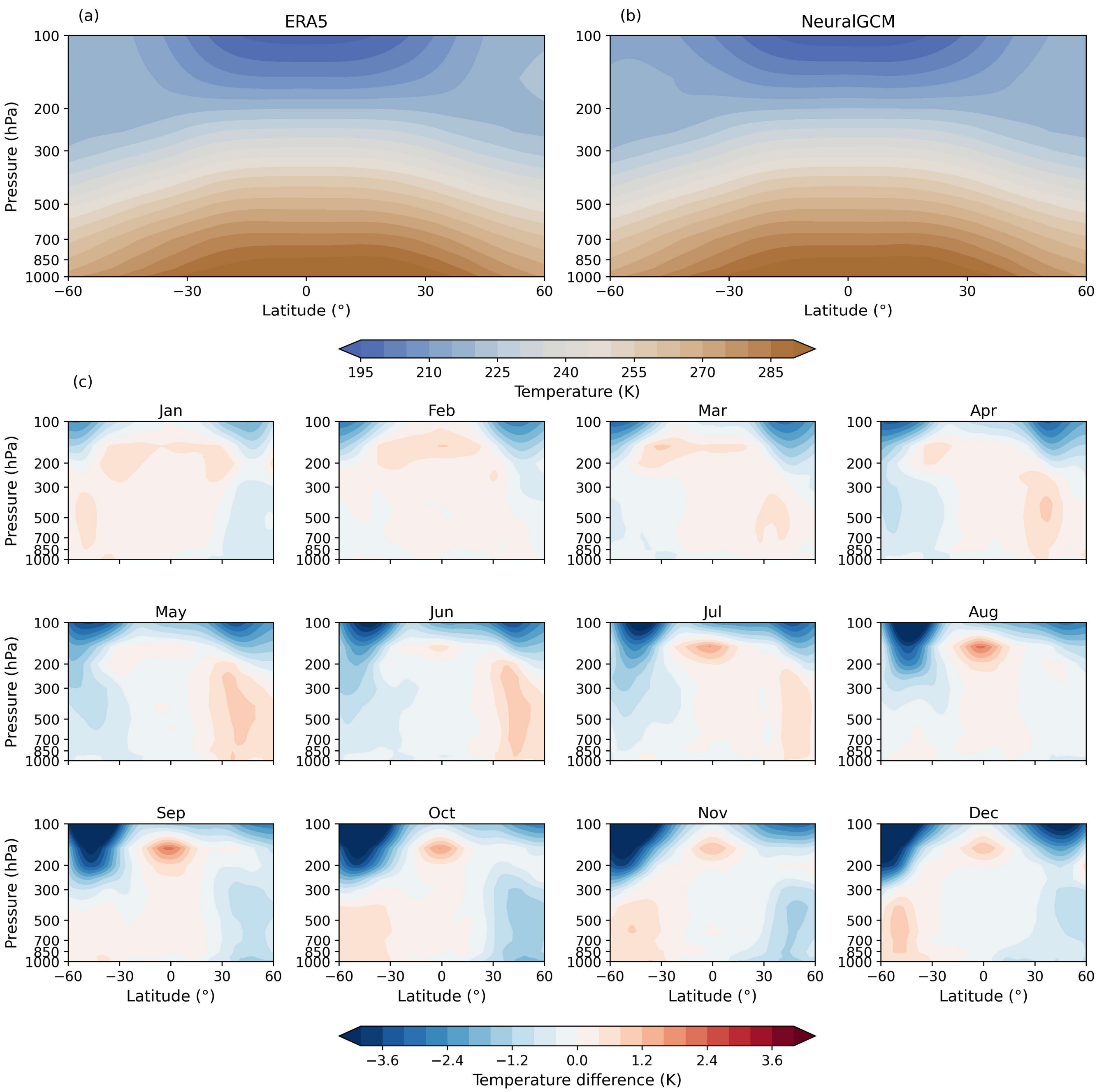

Figure S3. Meridional temperature profiles in ERA5 and NeuralGCM. (a,b) 1980–2022 mean pressure–latitude temperature profiles from (a) ERA5 and (b) the NeuralGCM ensemble mean. (c) Monthly NeuralGCM minus ERA5 temperature differences.

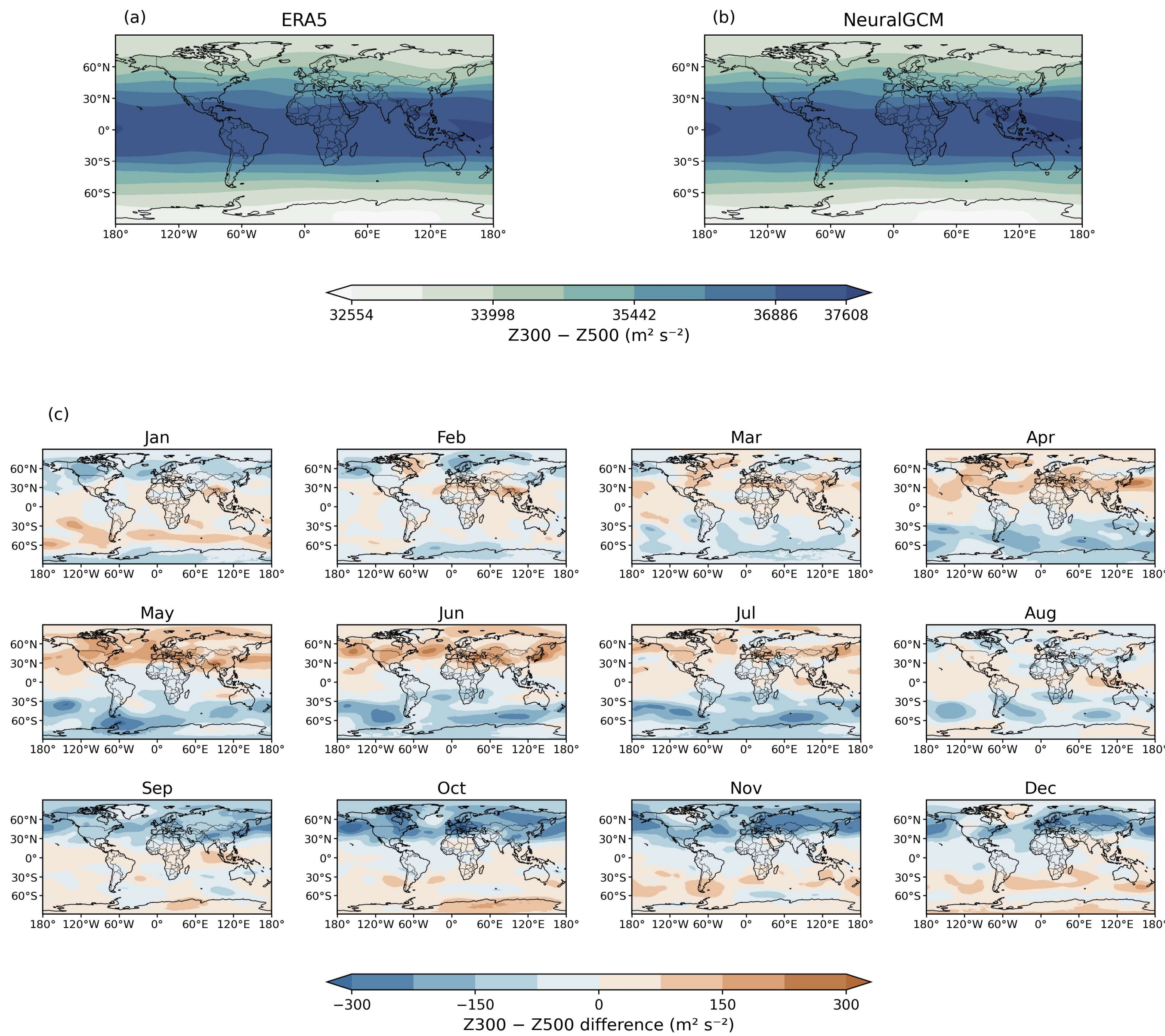

Figure S4. Geopotential difference between 300 hPa and 500 hPa in ERA5 and NeuralGCM. (a,b) The 1980–2022 mean Z300-Z500 from (a) ERA5 and (b) the NeuralGCM ensemble mean. (c) Monthly NeuralGCM minus ERA5 differences in Z300-Z500.

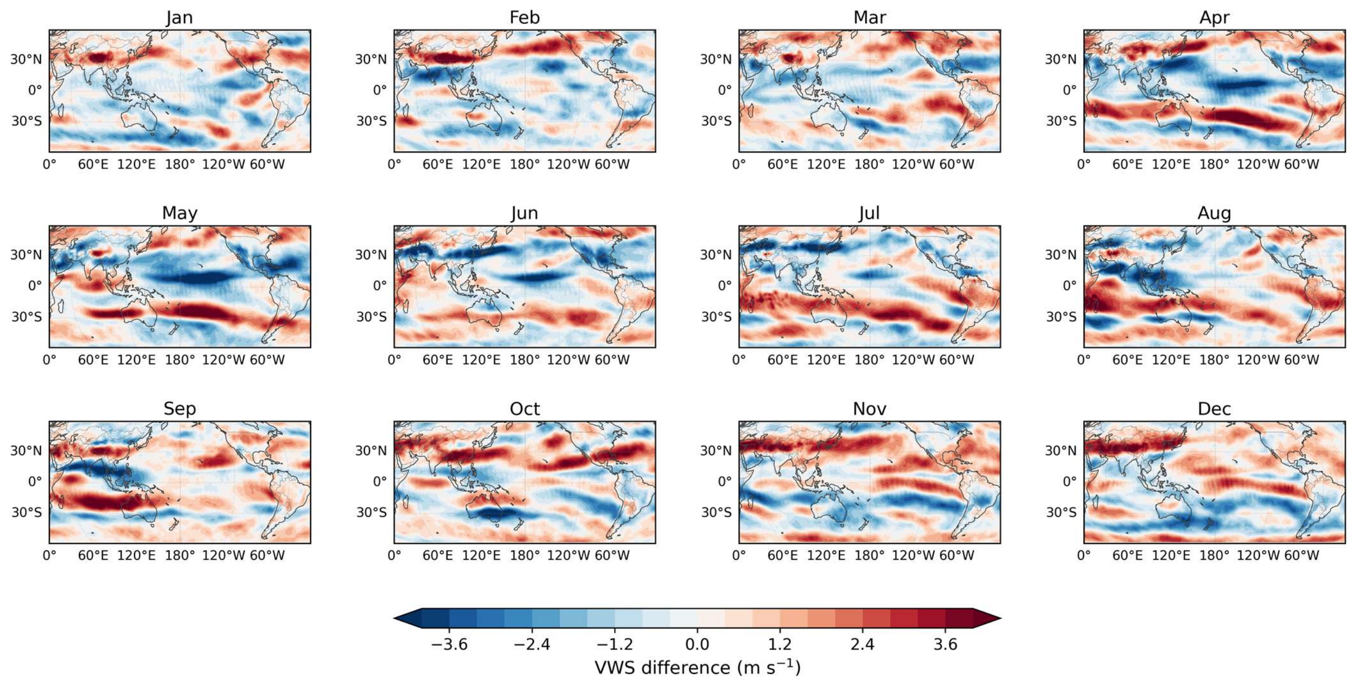

Figure S5. Monthly mean NeuralGCM minus ERA5 differences in 200–850-hPa vertical wind shear (VWS) over 1980–2022.

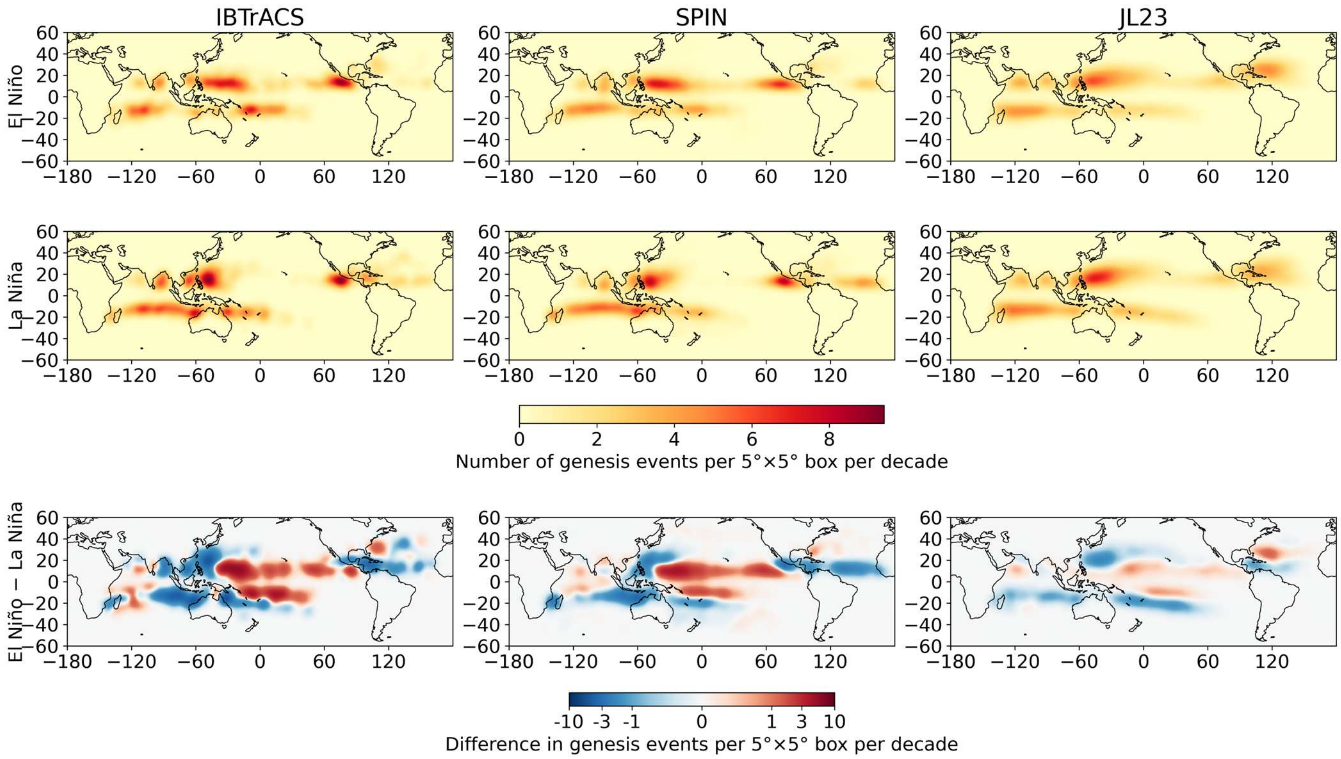

Figure S6. TC genesis counts in 5° × 5° grid boxes per decade from IBTrACS, SPIN and JL23 during 1980-2022. JL23 genesis densities are shown after applying a constant global scaling factor so that the total JL23 genesis count over 1980–2022 matches that of IBTrACS. Top and middle rows show genesis counts during El Niño-like and La Niña-like months, respectively, defined using the Niño 3.4 SST index with thresholds of +1σ and −1σ. The bottom row shows the El Niño minus La Niña difference in genesis counts per decade. The colour scale is linear between −1 and 1 and logarithmic for absolute differences greater than 1.

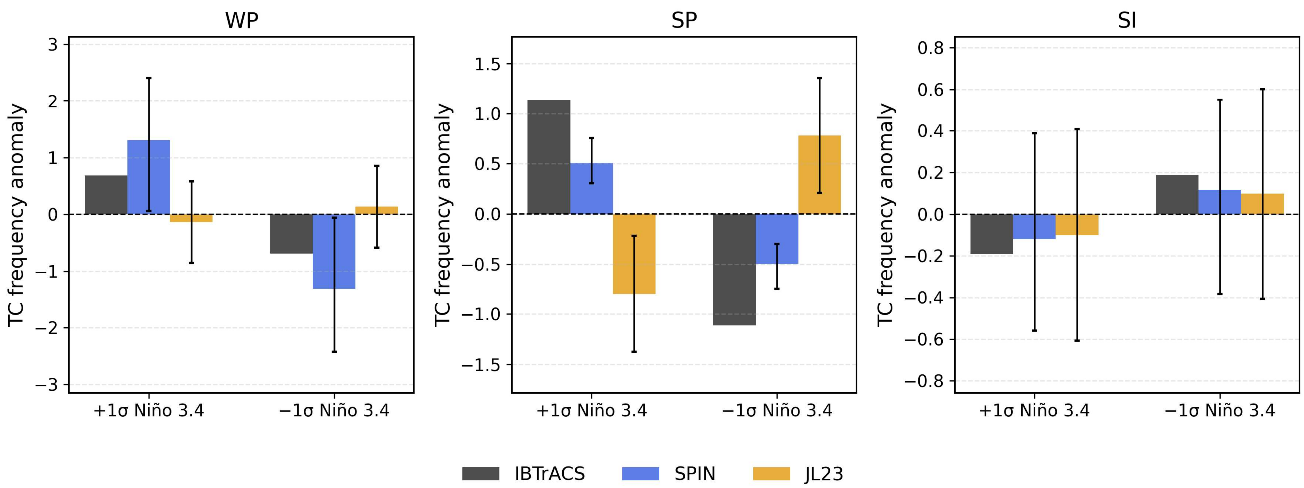

Figure S7. ENSO modulation of TC frequency in the WP, SP and SI basins. Bars show the TC frequency anomalies expected under +1σ (El Niño-like) and −1σ (La Niña-like) Niño 3.4 conditions, estimated from the linear relationship between TC frequency anomalies and the Niño 3.4 index over 1980–2022. TC frequency and Niño 3.4 index are calculated over May–December for the WP basin and December–April for the SP and SI basins. TC anomalies are expressed relative to each dataset's own climatology. Error bars show the 10th–90th percentile range across SPIN ensemble members and the 95% ordinary least squares (OLS) confidence interval for JL23. JL23 counts are scaled separately within each basin so that the total JL23 TC count in each basin matches that of IBTrACS.

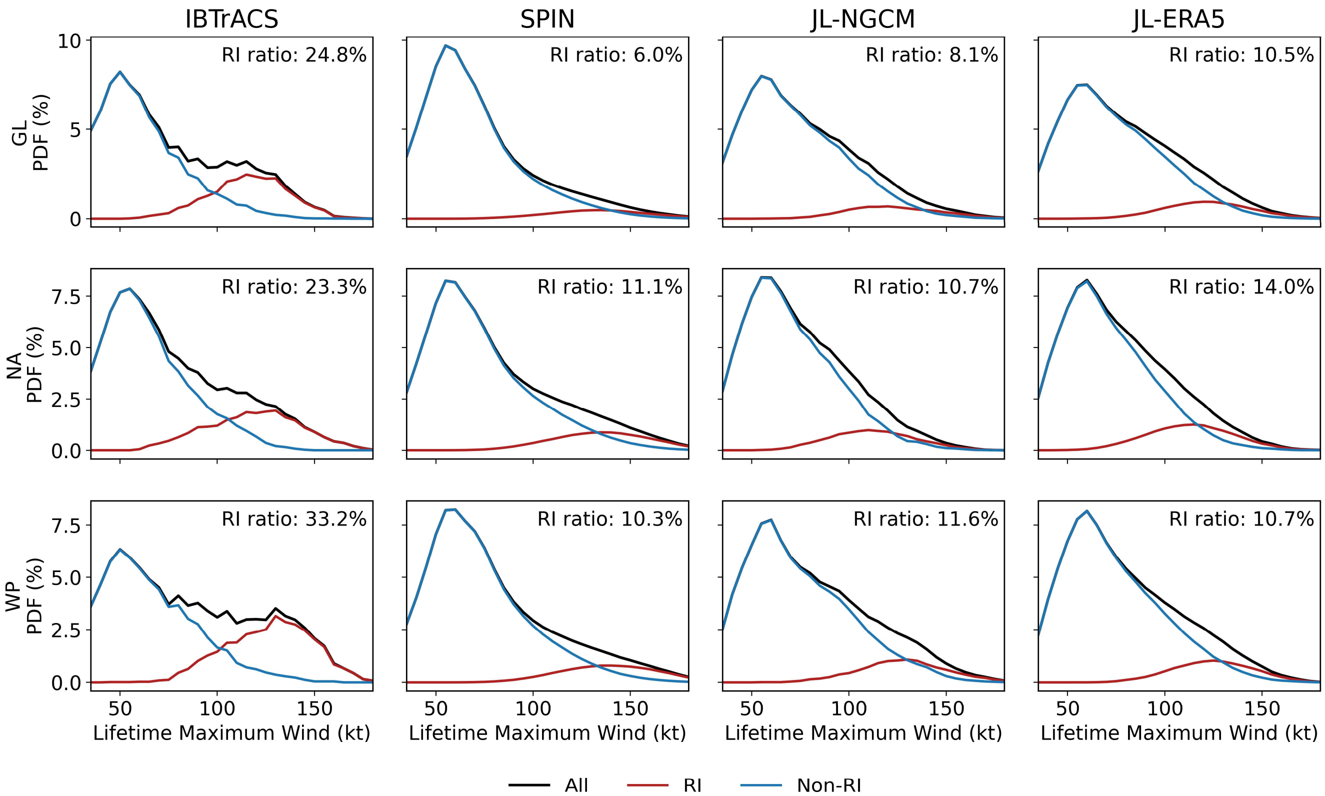

Figure S8. Distributions of TC lifetime maximum intensity (LMI) for rapid intensification (RI) and non-RI cases (1980–2022). Columns show IBTrACS, SPIN ensemble mean, JL23-downscaled NeuralGCM, and JL23-downscaled ERA5. For both JL-downscaled NeuralGCM and ERA5, the number of TCs is obtained by sub-sampling the downscaling events to match the number of observed events. Rows correspond to GL, NA, and WP basins. RI ratios are given in the upper-right of each panel.

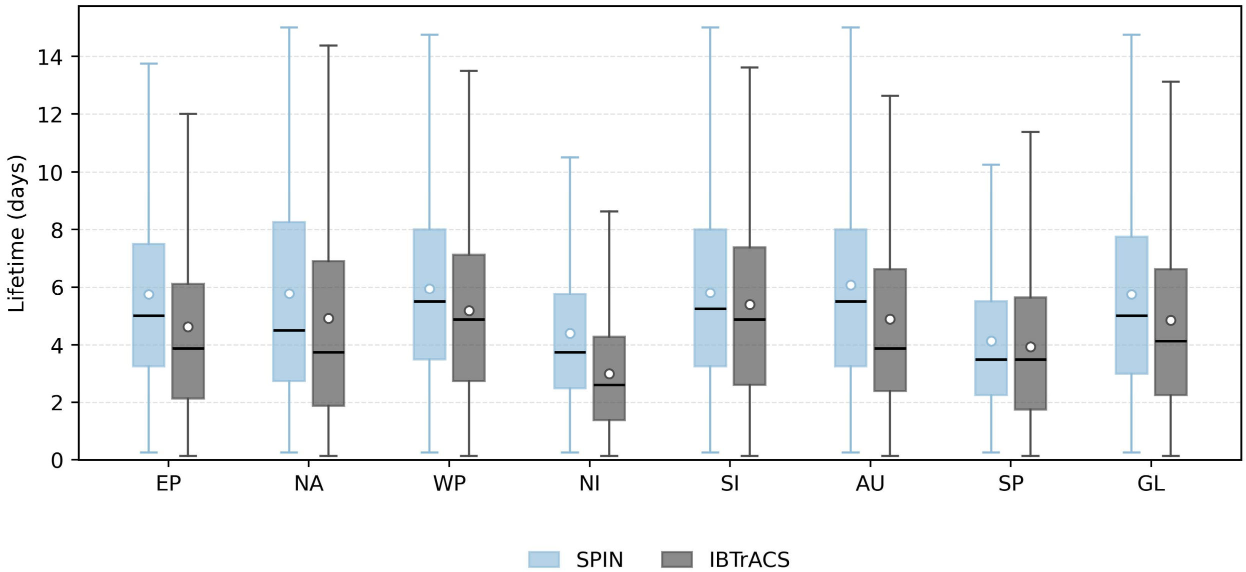

Figure S9. Comparison of TC lifetime from 1980–2022 between IBTrACS and the SPIN ensembles across basins. Boxes indicate the interquartile range, horizontal lines denote the median, whiskers extend to 1.5 times the interquartile range, and circles indicate the mean.

Basin	Model	$D_{\mathrm{KL}}(O \parallel M)$	ACDFs
GL	SPIN	0.070	3.414
	JL-ERA5	0.042	-1.146
	JL-NGCM	0.038	-4.497
NA	SPIN	0.015	-2.582
	JL-ERA5	0.030	0.121
	JL-NGCM	0.029	-3.821
WP	SPIN	0.085	8.431
	JL-ERA5	0.101	9.389
	JL-NGCM	0.048	5.693

Table S1. Evaluation of model-simulated LMI (1980-2022) using the Kullback–Leibler (KL) divergence $D_{\mathrm{KL}}(O \parallel M)$ and the area between cumulative distribution functions (ACDFs) of the model and observations, shown across basins for SPIN, JL23-downscaled ERA5, and JL23-downscaled NeuralGCM.

Basin	Model	$D_{\mathrm{KL}}(O \parallel M)$	ACDFs	ACDFs (0-5 day)
EP	SPIN	0.023	0.78	0.17
	IBTrACS (uniform)	0.033	0.42	0.47
NA	SPIN	0.017	0.62	-0.08
	IBTrACS (uniform)	0.019	1.33	0.28
WP	SPIN	0.014	-0.55	-0.08
	IBTrACS (uniform)	0.031	0.58	0.48
NI	SPIN	0.069	-2.48	-0.2
	IBTrACS (uniform)	0.182	5.37	0.63
SI	SPIN	0.015	0.7	0.12
	IBTrACS (uniform)	0.057	1.96	0.5
AU	SPIN	0.012	-0.26	-0.18
	IBTrACS (uniform)	0.033	1.32	0.25
SP	SPIN	0.048	-1.5	-0.19
	IBTrACS (uniform)	0.074	3.13	0.27

Table S2. Evaluation of model-simulated TC inter-genesis dates (1980-2022) using the Kullback–Leibler (KL) divergence $D_{\mathrm{KL}}(O \parallel M)$, and the area between cumulative distribution functions (ACDFs) of the model and observations for all bins and 0-5day bin. Results are shown across basins for SPIN and IBTrACS with uniformly sampled dates.